LAWRENCE
LIVERMORE
NATIONAL
LABORATORY

LLNL-PROC-583112

Visualization of ELM dynamics and response to external magnetic perturbations via 2D Electron Cyclotron Emission Imaging in KSTAR

H. K. Park

September 19, 2012

24th IAEA FEC
San Diego, CA, United States
October 8, 2012 through October 13, 2012

Disclaimer

Visualization of ELM dynamics and response to external magnetic perturbations via 2D Electron Cyclotron Emission Imaging in KSTAR

H.K. Park[a], M.J. Choi[a], J. Lee[a], W. Lee[a], G.S. Yun[a], Y.S. Bae[b], Y.M. Jeon[b], J.H. Lee[b], S.W. Yoon[b], C.W. Domier[c], N.C. Luhmann, Jr. [c], A.J.H. Donné[d,e], W.W. Xiao [b,f], I. Joseph[g], W. Meyer[g], X.Q. Xu[g], and KSTAR Team[b]

[a]*POSTECH, Pohang, Korea*
[b]*NFRI, Daejeon, Korea*
[c]*UCD, Davis, USA*
[d]*FOM-Institute, DIFFER, The Netherands*
[e]*Einhoven Univ. of Tech., Dept. of Appl. Phys., The Netherlands*
[f]*SWIP, Chengdu, China*
[g]*LLNL, CA, USA*
e-mail: hyeonpark@postech.ac.kr

Abstract. Enhanced physical understanding of the nature of the Edge Localized Mode (ELM) instability in the H-mode regime of toroidal plasmas requires advanced diagnostic tools in order o better visualize their dynamics. A high spatial and temporal resolution 2-D Electron Cyclotron Emission Imaging (ECEI) system[1] was utilized successfully characterize the real time dynamics of ELMs[2] including the growth, saturation and bursting process of this instability during two campaigns (2010 and 2011) of the Korean Superconducting Tokamak Advanced Research (KSTAR) device. It is particularly important to find a comprehensive way to eliminate or supress this instability, which is a critical issue for H-mode operation in ITER. During the 2011 campaign, both Resonant Magnetic Perturbation (RMP) coils with toroidal mode *n=1* perturbations[3] and Supersonic Molecular Beam Injection (SMBI) were introduced to control the ELMs. The detailed temporal and spatial response of the ELMs to the RMP and SMBI were visualized. The stationary 2D ELM image at the saturated regime is directly compared with that from numerical simulation. During the 2012 campaign, 3D visualization will address many critical issues such as toroidal asymmetry related to the dynamics of suppression and mitigation of ELMs.

1. Introduction

Edge-localized modes (ELMs) are ubiquitous in the high confinement mode (H-mode) of a tokamak plasma, where the edge pressure gradient is large over a short physical distance near the separatrix, and have been extensively studied in many tokamak devices[3-10] for the last three decades since their first observation in ASDEX [11]. The H-mode was adopted as a standard mode of operation in ITER, yet large ELMs can severely limit the life time of the divertor; thus, understanding and control of this instability became an essential research subject for all divertor tokamaks. A control system that requires actively cooled current carrying in-vessel structures are difficult to engineer for not only for ITER but also for future devices, such as a DEMO facility. Therefore, it is desirable to develop a control technique that is both effective and relatively simple to engineer. The physical mechanism of onset of these instabilities appears to be based on the peeling/ballooning mode which is a combination of two classical instabilities: the ballooning mode driven by the steep pressure gradient at the edge [pedestal] of the H-mode plasmas and the peeling mode driven by the edge current density largely due to the bootstrap current at the last closed flux surface. The nonlinear behavior including the bursting of the mode, which

appears to be localized in toroidal plane, is still under investigation. Numerous control methods have been studied including resonant magnetic perturbation (RMP) coil designs [various *n* numbers], massive gas injection [including both supersonic molecular beam and solid pellets], and local edge current perturbations [by Electron Cyclotron Current Drive]; however, there currently is no clear consensus on the optimum control method. The phenomenology of the ELM is multi-dimensional (a combination of global symmetry and local asymmetric transient behaviors) and responses from various control methods are even more complex. Consequently, in order to develop a comprehensive physical model and "smart" control method for the ELMs, it is essential to measure 2D and/or 3D images with adequate temporal and spatial resolution. Following the first real time visualization of the core *m=1* physics with the Electron Cyclotron Emission Imaging system on TEXTOR[12], the technique has been successfully translated to the ELM physics study in AUG[13, 14] and KSTAR[2]. During the KSTAR campaigns of 2010 and 2011, both stationary images as well as dynamic images such as the ELM growth from the initiation phase to burst were successfully documented. Over the 2011 KSTAR campaign, among several control methods[15,16], the RMP[17] and SMBI have demonstrated successful suppression and mitigation of the ELMs on KSTAR. In this paper, the entire process of the suppression and mitigation phase (mode intensity, radial and poloidal structure, etc.) was also visualized in 2D. The 2D image in the saturated regime is compared with the numerical simulation results from the BOUT++ code [18,19] and the observation will be compared with theoretical models. Also the future plan for 3D imaging and critical physics to be assessed is included.

2. ELM Dynamics on KSTAR

2.1 Visualization using the High Resolution 2D ECEI System

The electron cyclotron emission imaging (ECEI) technique is based on established heterodyne radiometry for the measurement of the electron cyclotron emission (ECE) intensity from the magnetically confined optically thick plasmas, in which the emission intensity (I_{rad}) is proportional to the local electron temperature (T_e); $I_{rad}(R) = \alpha T_e(R)$, where α is a calibration factor. Utilizing a vertical detector array and large optics which collects the emission to form an image on the detector plane, the first real time 2D ECEI system was successfully tested on TEXTOR. Following this work, a number of tokamaks have successively implemented more advanced ECEI systems that have contributed to the physics understanding of sawteeth, tearing modes, and Alfvén eigenmodes through direct comparative studies with the predicted images from theoretical models. However, application of the ECE measurement to edge plasmas in the medium performance plasmas in which the optical thickness is marginal requires careful attention in the analysis of the measured emission. Under such edge plasma conditions, the measured emission intensity may not represent the local T_e; however, localization of the measurement is still valid with a slightly broadened spatial resolution. If the optical thickness falls further, then the measurement is no longer localized. Optical depth issues related to these problems for the plasma close to the last closed flux surface are discussed, when the ECEI system was applied to the edge plasmas in AUG[13]. The ECEI system on KSTAR consists of two independent receiver arrays and large aperture optics with zooming capability as illustrated in Fig. 1, providing a simultaneous measurement of two independent regions along the field of view as shown in this figure. The two viewing areas, which correspond to the

individual receiver arrays as denoted by HFS (high-field side) and LFS (low-field side) in the figure, can be placed anywhere in the poloidal cross-section with a variable vertical coverage from ~30 to ~90 cm owing to the wide-band (85–145 GHz) microwave heterodyne detection technologies and the optimized zooming and focusing capabilities of the optics. This flexibility has allowed various combinations of HFS and LFS view positions, providing excellent opportunities to study a variety of plasma instabilities and turbulence phenomena in 2D such as sawteeth, tearing modes, ELMs, and turbulent fluctuations during the H-mode transition. Each detector array provides 24 (vertical) x 8 (radial) = 192 local emission measurements with a spatial resolution ~1–2 cm and a time resolution down to ~1 μs. The detector arrays are optimized for the extraordinary (X) mode 2nd harmonic ECE at B_o~2T (corresponding to the magnetic field at the major radius R_o = 1.8 m).

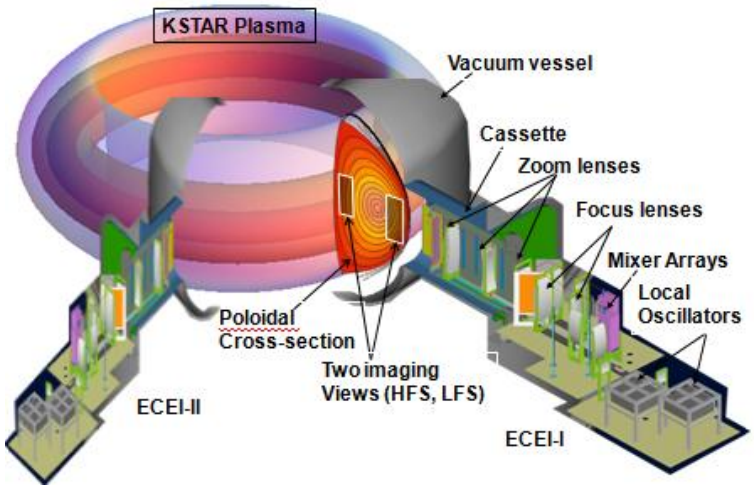

Fig.1. 3D schematic of the two ECEI systems on KSTAR. The ECEI-I system has been successfully operated for the 2010 and 2011 campaigns. The second system (ECEI-II) will be commissioned during the 2012 campaign to directly measure toroidal uniformity of the mode structure, magnetic shear of the ELMs and rotation speeds (toroidal, poloidal and flow).

In KSTAR H-mode operation, the detailed dynamics of ELMs were studied via a 2-D ECEI system which is capable of simultaneously visualizing the core and edge MHD instabilites. Figure 2 shows an example of the dynamics of the ELM filaments captured in the edge in KSTAR. The image is plotted on the $\Delta I_{rad}/\langle I_{rad}\rangle$ scale, where $\langle I_{rad}\rangle$ denotes a time average and $\Delta I_{rad} = I_{rad} - \langle I_{rad}\rangle$. Note that the observed rotation of the ELM filaments is counterclockwise (electron diamagnetic drift direction) in the ECEI view in opposition to the clockwise rotation of the core *m=1* mode, indicating that the rotation speed consists of more than solid body rotation. This issue will be one of the challenges in the 2012 KSTAR campaign with the aid of the second ECEI-II system which is located at an adjacent port (22.5^0 apart) as illustrated in Fig.1. The 3D data will be used not only for clarifying the rotation speed of the ELMs (mixture of toroidal, poloidal and flow) but also to assess the toroidal uniformity of the mode due to possible mode competition and magnetic shear. The experimentally observed ELM dynamics revealed a semi-exponential growth rate of ~100 μs before it is saturated as shown in Fig.2. During the saturation phase, the observed rotation speed was ~1km/s in the electron diamagnetic direction. After a relatively long saturation period of ~10 ms where the average mode size does not grow, the mode bursts outward as shown in

Fig. 2. The bursting process is observed to be highly non-linear and localized in the poloidal and toroidal planes. Here, the filament structure is first poloidally elongated and a pressure finger grows out prior to the fast burst (~100 μs) which is an indication of a magnetic reconnection process as shown in Fig. 2. Multiple small bursts often follow the large initial burst.

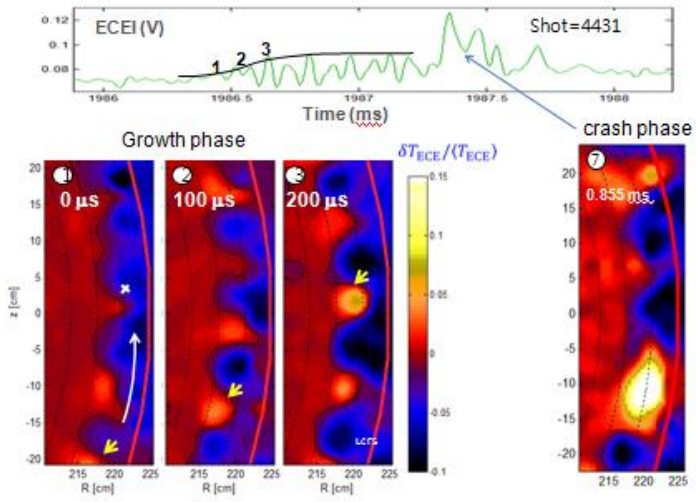

Fig.2. Dynamics of ELMs: Time traces of a single ELM event and the corresponding 2D images at different times. Growth saturates at about ~100 μs. and the bursting behaviour of each tube is irregular with the bursting time scale being comparable to the magnetic reconnection time scale.

2.2 Comparison of the measured 2D image with BOUT++ simulations

The measured 2D image of the ELM for n~5 has a radial size of ~3cm and a poloidal mode spacing of ~22cm (peak to peak) as shown in Fig.3a. In the BOUT++ simulation[18,19], the positively determined toroidal mode number (*n*~5) by magnetic probe is used to obtain an optimum growth rate for various pressure profiles based on the measured T_e profile and the line average density. The narrow radial extent of the ELM mode structure (~1cm) is maximized with the relaxed pressure profile that allows a solution with a finite growth rate. Here the radial width of the mode was increased from ~1cm to ~1.5 cm. Then the poloidal mode spacing of the calculated mode was adjusted with various edge q profiles until the poloidal mode spacing is close to that of the measured image (~22cm, peak to peak). In the course of this exercise, it was found that the poloidal mode spacing driven by the same toroidal mode number (n~5 for this case) is extremely sensitive to the local q-value. The local q value at R=222 cm (ρ~0.85) was varied from ~5 to ~8 while the poloidal mode spacing was changed from ~40 cm to ~22 cm. Note that there are other possible solutions that agree with the measurement for adjacent *n* numbers with different q profiles. Considering that the radial extent of the simulated ELM mode is comparable to the instrumental resolution of the system as shown in Fig.3b, one would expect that the measured image will be broadened. In fact, there are two broadening effects which should be imposed to compare the calculated image with the measured one. The first one is the emission broadening which occurs when the optical depth is marginal. The other is instrumental broadening when the target size is comparable to the instrumental width (i.e. the antenna pattern of each detector). The synthetic image

deduced from the simulation result with tightly constrained pressure and q profiles is in a good agreement with the measurement as shown in Fig. 3a.

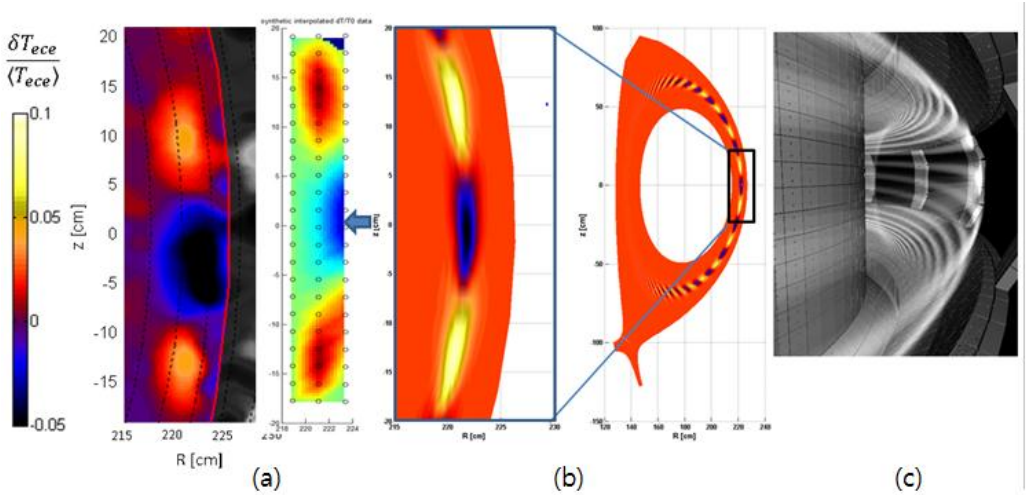

Fig.3. (a) Synthetic image is directly compared with the experimentally measured 2D images. (b) The simulated 2D image from the BOUT++ code (in the middle) is further processed considering the emissivity and instrumental broadening. (c) Simulation result for the ELM with n~5 is plotted against the KSTAR in-vessel structure

3. Response of the ELMs to External Perturbations

Empirical attempts to control the ELM instability have been undertaken in the majority of present-day tokamaks. Over the KSTAR 2011 campaign, significant efforts were made to control ELMs. The main approach was RMP with the In-Vessel Control Coils (IVCC) with *n=1* magnetic perturbations. In addition to this, SMBI, ECH/ECCD, and plasma bouncing have been introduced to control the ELMs. The response for these methods ranged from no response to full suppression. In this section, the entire time evolution of the responses of the ELMs during RMP and SMBI will be discussed.

3.1 Characteristics of the ELM response during RMP experiments

It is important to understand the role of the RMP in the suppression of ELMs[17]. In the KSTAR experiment, ELMs with toroidal mode number of n~10 with a moderate intensity were observed before the RMP is applied in the H-mode phase (A), as shown in Fig.3. Here, the RMP with *n=1* configuration was applied at 3s and the detailed control coil configuration for this experiment can be found in Refs. [15,16]. As the RMP is applied, the first notable change was that the frequency of the smaller ELMs increased from 6 to 8 kHz at 3.19s as shown in Fig. 3c. The change in the frequency is due to the increase in plasma rotation, because there were no changes in the poloidal spacing of the ELMs observed in the 2D images. During the intermediate phase (B) in this figure, the ELM size is increased with an altered mode number. The first larger ELM appeared at ~3.3s and the measured mode number was changed from *n~10* to *n~5*. Here, *n~10* is inferred from the observed poloidal mode spacing in the 2-D images in both phases [images A and B in (b)], while the magnetic probe measurement confirmed *n~5* for the large ELMs. Then a low order mode (*n~5*) appeared after a relatively long period of quiescence (~30 ms), after the last burst of the *n~10* mode ELM. During the quiescent period, the edge pressure profile becomes steeper; the ECEI channel in the vicinity of the last closed flux surface (ch#3) is

unchanged whereas the channels (#4 and #5) near the pedestal region are increased steadily as shown in Fig.3a. Note that the line average density is steadily falling during phase B. This is consistent with the previous observation[8] that the mode becomes more peeling-like as the edge current density is increased due to the increased pressure gradient. Also the collisionality decreased as the edge electron density decreases. Then, the first large ELM (*n~5*) appears suddenly and continues up to ~3.95 s, when the ELMs are finally suppressed. Here, the *n~10* mode reappeared after the crash of the *n~10* mode for a while in phase B.

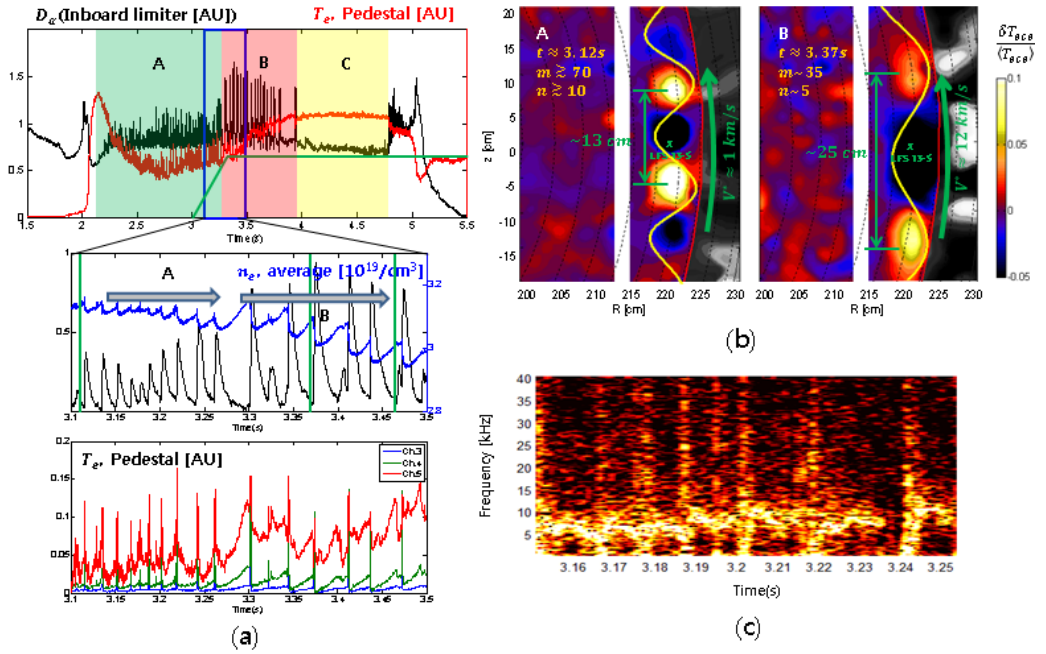

Fig.3. The time evolution of the ELM during the RMP experiment. (a) Time evolution of ELMs with D_α signal and pedestal T_e. (Original ELM phase (A), intermediate phase (B) and suppression phase (C).(b) Image of the ELM before the RMP power is applied (A), intensified ELM image during RMP phase(B), (c)-Initial frequency response due to RMP.

If the altered state of the ELM (from *n~10* to *n~5*) and suppression itself during the RMP arise from competition between the magnetic island structure of the ELMs and the applied *n=1* RMP perturbation, then one would expect to observe the initial interference between the two competing modes on a time scale of the magnetic field diffusion. There was no notable observation of such interference. The RMP with the *n=1* magnetic perturbation may have modified the plasma equilibrium and/or radial transport which affected the edge pressure profile so that the lower n mode (~5) can be excited with the increased edge current density due to the steepened pressure gradient and reduced collisionality. Here, further analysis of the bootstrap current and accurate measurements of the edge pressure gradient is required. Qualitatively, the observed T_e profile in phase B was steeper than that of phase A. Then it appears that the top of the pedestal expands radially from phase B to phase C. One possible explanation is that the steep gradient region becomes so narrow that the free energy that would be released by the ELM is smaller than the energy that must be invested in the narrow radial envelope of the mode.

3.2 ELM mitigation by SMBI

Figure 4 illustrates an indication of ELM by SMBI. Here, the time history of the

D_α for the ELM monitor and the corresponding ECEI images (b-d) for shot 6352 are provided. After SMBI, the ELM frequency increases from 28Hz to 68Hz and the amplitude is decreased. The core toroidal rotation, mostly due to the NBI torque is also decreased from ~140km/s to ~130km/s due to the reduction of the core heating beam during the ELM mitigation time, and then slowly recovers to ~138km/s as the NBI penetration is improved. The mitigation interval is about ~400ms, and the degradation of the stored energy is about 8%. Also, the line average density is increased by up to ~9% after SMBI. Three 2D images of the ELMs (before SMBI, during mitigation, and after mitigation) are shown in this figure. The arrows show the direction of poloidal rotation at the plasma edge, which is in the electron diamagnetic direction. In Fig.4 (b), (c) and (d), the poloidal spacing of the mode for each case is marked as L1, L2, and L3. Here, the *n~6* mode is increased to n~9 and then decreased to n~7. The increase in *n* number from 6 to 9 can be interpreted as the effect of increased collisionality in the peeling/ballooning mode model.

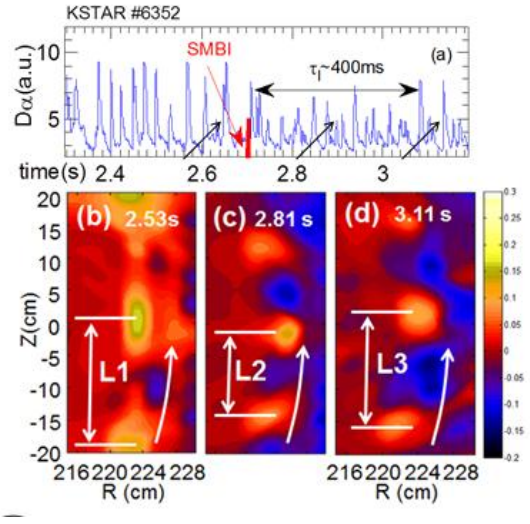

Fig.4 The time evolution of the ELM during SMBI experiment. (a) D_α signal (b) Image of the ELM prior to the SMBI (c) ELM structure during the SMBI (d) Recovery phase of the ELM

4. Summary

The dynamics of ELMs in H-mode plasmas including their growth, saturation, and outburst, were observed using the 2D ECEI system on KSTAR. In the RMP experiment, the ELMs were suppressed through the intermediate phase, where the mode number was changed from n~10 to n~5 with increased intensity as the RMP was applied. This change of the mode is consistent with the peeling/ballooning mode model in which the mode is moved from the ballooning dominated regime to the peeling dominated regime as the edge current density driven by bootstrap current (from the steepened pressure gradient) is increased and the decreased collisionality due to the decreased density. The simulation 2D image from the BOUT++ code was in good agreement with the measured 2D image. In the SMBI case, while the ELM is mitigated, the change of the mode number from n~6 to n~9 and back to n~7 as the electron density is changed can be interpreted as the effect of collisionality. Transient asymmetry due to the multiple toroidal mode competition, complex rotation issue and locality of bursting behavior will be clarified by the 3D imaging in the 2012 campaign.

Acknowledgment

This work is supported by NRF of Korea contract No. 20090082507 and BK21, US DOE Grants DEFG02-99ER54531 & DEAC52-07NA27344, NWO, and EURATOM

References

[1] Yun, G.S., et al., "Development of KSTAR ECE Imaging System for Measurement of Temperature Fluctuations and Edge Density Fluctuations", Rev. Sci. Instrum. **81**, 10D930 (2010).
[2] Yun, G.S., et al., "Two-Dimensional Visualization of Growth and Burst of the Edge-Localized Filaments in KSTAR H-mode Plasmas", Phys. Rev. Lett. **107**, 045004 (2011).
[3] Kirk, A., et al., "Spatial and Temporal Structure of Edge-Localized Modes", Phys. Rev. Lett. **92**, 245002 (2004).
[4] Kirk, A., et al., "Evolution of Filament Structures during Edge-Localized Modes in the MAST Tokamak", Phys. Rev. Lett. **96**, 185001 (2006).
[5] Josheph, I, "Edge-Localized Mode Control and Trnasport gEnerated by Externally Applied Magnetic Perturbations", Contrib. Plasma Phys., **52**, 326-347 (2012)
[6] Schmid, A., et al., "Experimental Observation of the Radial Propagation of ELM Induced Filaments on ASDEX Upgrade", Plasma Phys. Controlled Fusion **50**, 045007 (2008).
[7] Silva, C., et al., "Reciprocating Probe Measurements of ELM Filaments on JET", Plasma Phys. Controlled Fusion **51**,105001 (2009).
[8] Osborne, T.H., et al., "Edge stability of stationary ELM-suppressed regimes on DIII-D", J. Phys. Conf. Series, **123** 012014 (2008)
[9] Maqueda, R.J., Maingi, R., and NSTX Team, "Primary Edge Localized Mode Filament Structure in the National Spherical Torus Experiment", Phys. Plasmas **16**, 056117 (2009).
[10] Terry, J.L., et al., "The Dynamics and Structure of Edge-Localized-Modes in Alcator C-Mod", J. Nucl. Mater. **363–365**, 994 (2007).
[11] Wagner, F., et al., "Regime of Improved Confinement and High Beta in Neutral-Beam-Heated Divertor Discharges of the ASDEX Tokamak", Phys. Rev. Lett. **49**, 1408, (1982).
[12] Park, H.K., et al., "Observation of High-Field-Side Crash and Heat Transfer during Sawtooth Oscillation in Magnetically Confined Plasmas", Phys. Rev. Lett. **96**, 195003, (2006).
[13] BOOM, J.E., et al., "2D ECE measurements of type-I edge localized modes at ASDEX Upgrade", Nucl. Fusion, **51** 103039, (2011)
[14] Classsen, I.G.J., et al., "Characterization of temperature fluctuations during type-I and type –II edge localized modes at ASDEX Ugrade", EX/P4-07, ibid, (2012)
[15] Kim, J., et al., "ELM control experiments in the KSTAR device", Nucl. Fusion **52,** (2012) 000000, (2012)
[16] Jeon, Y.M., et al., "Suppression of Edge Localized Modes in High-confinement KSTAR Plasmas by Nonaxisymmetric Magnetic Perturbations", Phys. Rev. Lett. **109**, 035004 (2012).
[17] Snyder, P.B., et al., "The EPED pedestal model and edge localized mode-suppressed regimes" Phys. of Plasmas, **19**, 056115 (2012)
[18] Xu, X.Q., et al., "Nonlinear ELM simulations based on a nonideal peeling–ballooning model using the BOUT++ code" , Nucl. Fusion, **51,** 103040 (2011) .
[19] Dudson, B.D., et al., **"**A framework for parallel plasma fluid simulations", Computer Physics Communications, **180**, 1467 (2009)